ANESTHESIOLOGY

Dexmedetomidine Activation of Dopamine Neurons in the Ventral Tegmental Area Attenuates the Depth of Sedation in Mice

Gaolin Qiu, M.M., Ying Wu, M.M., Zeyong Yang, M.D., Ph.D., Long Li, M.M., Xiaona Zhu, Ph.D., Yiqiao Wang, M.D., Ph.D., Wenzhi Sun, Ph.D., Hailong Dong, M.D., Ph.D., Yuanhai Li, M.D., Ph.D., Ji Hu, Ph.D.

ANESTHESIOLOGY 2020; 133:377–92

EDITOR'S PERSPECTIVE

What We Already Know about This Topic

- Dexmedetomidine is a highly selective α2 receptor agonist with unique sedative properties
- Dopaminergic neurons in the ventral tegmental area express α2 receptors, and activation of these cells induces recovery from anesthesia
- The effects of dexmedetomidine on dopaminergic neurons of the ventral tegmental area are incompletely understood

What This Article Tells Us That Is New

- Dexmedetomidine, *via* α2 receptor–dependent mechanisms, induces activation of dopaminergic neurons in the ventral tegmental area of adult mice
- Chemogenetic approaches together with electroencephalographic recordings reveal that the activation of dopaminergic neurons in the ventral tegmental area may contribute to rapid arousability during dexmedetomidine sedation

ABSTRACT

Background: Dexmedetomidine induces a sedative response that is associated with rapid arousal. To elucidate the underlying mechanisms, the authors hypothesized that dexmedetomidine increases the activity of dopaminergic neurons in the ventral tegmental area, and that this action contributes to the unique sedative properties of dexmedetomidine.

Methods: Only male mice were used. The activity of ventral tegmental area dopamine neurons was measured by a genetically encoded Ca^{2+} indicator and patch-clamp recording. Dopamine neurotransmitter dynamics in the medial prefrontal cortex and nucleus accumbens were measured by a genetically encoded dopamine sensor. Ventral tegmental area dopamine neurons were inhibited or activated by a chemogenetic approach, and the depth of sedation was estimated by electroencephalography.

Results: Ca^{2+} signals in dopamine neurons in the ventral tegmental area increased after intraperitoneal injection of dexmedetomidine (40 μg/kg; dexmedetomidine, 16.917 [14.882; 21.748], median [25%; 75%], *vs.* saline, –0.745 [–1.547; 0.359], normalized data, $P = 0.001$; n = 6 mice). Dopamine transmission increased in the medial prefrontal cortex after intraperitoneal injection of dexmedetomidine (40 μg/kg; dexmedetomidine, 10.812 [9.713; 15.104], median [25%; 75%], *vs.* saline, –0.498 [–0.664; –0.355], normalized data, $P = 0.001$; n = 6 mice) and in the nucleus accumbens (dexmedetomidine, 8.543 [7.135; 11.828], median [25%; 75%], *vs.* saline, –0.329 [–1.220; –0.047], normalized data, $P = 0.001$; n = 6 mice). Chemogenetic inhibition or activation of ventral tegmental area dopamine neurons increased or decreased slow waves, respectively, after intraperitoneal injection of dexmedetomidine (40 μg/kg; delta wave: two-way repeated measures ANOVA, $F[2, 33] = 8.016$, $P = 0.002$; n = 12 mice; theta wave: two-way repeated measures ANOVA, $F[2, 33] = 22.800$, $P < 0.0001$; n = 12 mice).

Conclusions: Dexmedetomidine activates dopamine neurons in the ventral tegmental area and increases dopamine concentrations in the related forebrain projection areas. This mechanism may explain rapid arousability upon dexmedetomidine sedation.

(ANESTHESIOLOGY 2020; 133:377–92)

Dexmedetomidine is a highly selective α2 adrenoceptor agonist that exhibits a unique sedative characteristic associated with rapid arousal.[1] This sedative characteristic shares an outward feature with natural sleep.[2] It has been previously shown that dexmedetomidine acts on an endogenous sleep-promoting pathway to exert its sedative effects.[3,4] In quantitative electroencephalography (EEG) analyses, sleep spindles were similar during dexmedetomidine sedation and normal sleep.[5] However, Garrity *et al.* found that dexmedetomidine-induced sedation is characterized by behavioral, electroencephalographic, and immunohistochemical phenotypes that are distinctly different

Supplemental Digital Content is available for this article. Direct URL citations appear in the printed text and are available in both the HTML and PDF versions of this article. Links to the digital files are provided in the HTML text of this article on the Journal's Web site (www.anesthesiology.org). G.Q. and Y.W. contributed equally to this article.

Submitted for publication October 3, 2019. Accepted for publication April 9, 2020. Published online first on May 12, 2020. From the Department of Anesthesiology, First Affiliated Hospital of Anhui Medical University, Hefei, China (G.Q., Y.W., Y.L.); School of Life Science and Technology, ShanghaiTech University, Shanghai, China (X.Z., J.H.); Department of Anesthesiology and Perioperative Medicine, Xijing Hospital, The Fourth Military Medical University, Xi'an, Shanxi, China (L.L., H.D.); Chinese Institute for Brain Research, Beijing, China (W.S.); Department of Anesthesiology, International Peace Maternity and Child Health Hospital, Shanghai Jiao Tong University School of Medicine, Shanghai, China (Z.Y.); Department of Anesthesiology, Anhui No. 2 Provincial People's Hospital, Hefei, Anhui, China (Y.W.); and Coinnovation Center of Neuroregeneration, Nantong University, Nantong, China (J.H.).

Copyright © 2020, the American Society of Anesthesiologists, Inc. All Rights Reserved. Anesthesiology 2020; 133:377–92. DOI: 10.1097/ALN.0000000000003347

Copyright © 2020, the American Society of Anesthesiologists, Inc. Unauthorized reproduction of this article is prohibited.

<zdoi;. DOI: 10.1097/ALN.0000000000003347>

Downloaded from http://asa2.silverchair.com/anesthesiology/article-pdf/133/2/377/514505/20200800.0-00022.pdf by guest on 13 March 2024

from similar measures obtained during sleep.[6] Therefore, the sedation of dexmedetomidine and natural sleep are not two identical states. Based on this unique sedative characteristic, dexmedetomidine is widely used in neurosurgical procedures requiring "cooperative sedation" for intraoperative neurologic assessments.[7–9] Dexmedetomidine is also widely used in the intensive care unit in situations where the patients need to be calm but arousable and capable of communicating their needs.[10] It is commonly thought that the sedative effect of dexmedetomidine is due to its action on α2 adrenoceptors on the presynaptic membrane of norepinephrine neurons in the locus coeruleus, which reduces the release of the excitatory neurotransmitter norepinephrine throughout the brain through a Gi-coupled mechanism.[3,11] The sedative mechanism of dexmedetomidine has not yet been thoroughly studied. Sedation is a complex process involving different neurotransmitter systems, many brain regions, and a large number of neural circuits.[12,13] Whether there are other brain regions and neuronal circuits involved in the sedative mechanism of dexmedetomidine needs to be studied. The ventral tegmental area is an important part of the ascending arousal system, which plays a vital role in the regulation of sleep and arousal.[12,14,15] Many studies have reported that direct electrical stimulation of the ventral tegmental area or activation of dopamine neurons in the ventral tegmental area can induce recovery from general anesthesia.[16–18] Similarly, administration of a dopamine reuptake inhibitor such as methylphenidate[19,20] or activation of dopamine D1 receptors can also induce recovery from general anesthesia.[21] Conversely, inhibition of ventral tegmental area dopamine neurons has a role in promoting sleep.[18] Although a few studies used microdialysis and found that dexmedetomidine reduces dopamine neurotransmitter in the forebrain,[22–24] it remains unclear whether dexmedetomidine affects the excitability of ventral tegmental area dopamine neurons. We hypothesized that dexmedetomidine increases the activity of dopamine neurons in the ventral tegmental area and that this action contributes to the easy arousal property of this drug. Here, we used *in vivo* Ca^{2+} and dopamine neurotransmitter measurement, *in vitro* slice recording, chemogenetics, and EEG recording to approach this hypothesis.

Materials and Methods

Experimental Animals

Only male mice were used in these experiments. The procedures of the animal experiments in this study strictly followed institutional guidelines and governmental regulations. To ensure the welfare of the animals, we tried our best to replace, refine, and reduce the mice in our experiments, and we will follow this principle in future research. All experiments were approved by the Institutional Animal Care and Use Committee at ShanghaiTech University, Shanghai, China, and the Chinese Academy of Sciences, Shanghai, China. Adult male *DAT-Cre* knock-in mice (Stock No. 006660, Jackson Laboratory, China) and male C57BL/6J mice (Shanghai Model Organism, China) at 8 to 12 weeks of age were used in our experiments. Our experiments did not examine the effect of dexmedetomidine-induced sedation in mice of different sexes since we did not use female mice. Before all experiments were performed, all mice were in good health at a normal weight (22 to 28 g). After all experiments were completed, the remaining mice were euthanized by isoflurane. All mice were maintained under a reversed 12/12 h day/night cycle (light at night and dark at day) at 22 to 25°C with *ad libitum* access to rodent food. All experiments were performed between 9 AM and 9 PM.

See Supplemental Digital Content, table S1 (http://links.lww.com/ALN/C382), listing baseline characteristics of the experimental mice.

Virus Injection and Optic Fiber Implantation

AAV vectors containing the DIO-GFP, DIO-GCaMP6m (fluorescent calcium indicators), DIO-mCherry, DIO-hM4Di (Gi-coupled human M4 muscarinic receptor), DIO-hM3Dq (Gq-coupled human M3 muscarinic receptor), DA1m (G protein-coupled receptor-activation-based dopamine sensor) and DA1m-mut (mutant G protein-coupled receptor-activation-based dopamine sensor) constructs were packaged into the AAV2/9 serotype with titers of 1 to 5 × 10^{12} viral particles per milliliter. The surgical procedures generally followed our previous studies.[25] Briefly, after being deeply anesthetized with isoflurane in a small box, the mice were placed on the stereoscopic positioning instrument and were kept warm (37°C) with an electric heating pad (BrainKing Biotech, China). Anesthesia was kept constant with 1 to 1.5% isoflurane mixed with pure oxygen at a 1 l/min flow rate. After the scalp was cut open, 3% hydrogen peroxide was used to remove the fascia from the skull surface. The bregma and lambda points were used to adjust the mouse head to the horizontal position. A small window with a diameter of 300 to 500 μm was opened at the location of the point of virus injection and fiber implantation. The virus was injected at 100 nl/min for a total of 300 nl using a microsyringe pump (Nanoject III #3-000-207, Drummond, USA). After the injection, the injector was allowed to remain in place for 10 min. The injection points were as follows: ventral tegmental area (coordinates from bregma: −3.10 mm [anteroposterior], ±0.45 mm [mediolateral], −4.25 mm [dorsoventral]), medial prefrontal cortex (+1.60 mm [anteroposterior], ±0.30 mm [mediolateral], −1.90 mm [dorsoventral]) and nucleus accumbens (coordinates from bregma: +1.18 mm [anteroposterior], ±1.3 mm [mediolateral], −3.9 mm [dorsoventral]). Unilateral injections were performed for fiber photometry, but bilateral injections were performed for chemogenetic experiments. For the recording fiber implantations, the fiber (200-μm OD, 0.37 numerical aperture, Newdoon, China) was slowly inserted and implanted above the targeted brain areas at a

Downloaded from http://asa2.silverchair.com/anesthesiology/article-pdf/133/2/377/514505/20200800.0-00022.pdf by guest on 13 March 2024

Copyright © 2020, the American Society of Anesthesiologists, Inc. Unauthorized reproduction of this article is prohibited.

distance of 0.15 mm. Then, the optical fiber and skull were fixed with dental cement. After the dental cement was completely dried, the mice were removed from the stereoscopic positioning instrument and placed on an electric blanket to keep warm (37°C). After the mice had fully recovered, they were returned to their home cage.

Fiber Photometry Recording

Fiber recording also followed the procedures described in our previous studies.[25] We used a fiber photometry system including one light-emitting diode at 488 nm as an excitation laser, a dichroic mirror with a 505 to 544 emission filter, and a photomultiplier tube (R3896, Hamamatsu, Japan). The analog voltage signals were converted to digital signals by a Power 1401 digitizer and recorded by Spike2 software (CED, United Kingdom) at 100 Hz. An optical fiber (RJPSF2, Thorlabs, USA) with an integrated rotary joint that prevented fiber damage from the animal movement was used to guide the light between the fiber photometry system and the implanted optical fiber. The laser power was adjusted at the tip of the optical fiber to a low level of 20 to 40 μW to minimize bleaching. The recordings were made after the animals had recovered from surgery for 2 weeks. While recording, the mice were allowed to move freely in a white chamber (40 × 40 × 40 cm, length × width × height) for at least 1,000 s. Then, the mice were intraperitoneally injected with saline (10 μl/g), and the recording continued for another 1,200 s. After that, the mice were administered dexmedetomidine (10, 40, 100, or 400 μg/kg; 10 μl/g) and recorded for at least 6,000 s. The data were extracted and analyzed by MATLAB R2018b (MathWorks, USA). To normalize the data, the ΔF/F was calculated by (F – F0) / F0, where F0 is the baseline fluorescence signal averaged over a window of at least 20 s, and F is the real-time fluorescence signal. ΔF/F values were expressed as percentages (*i.e.*, multiplied by 100) and presented with average plots with a shaded area indicating the SD. To calculate the average response and increased duration in ΔF/F values, we first segmented the data based on behavioral events. Then, we calculated the average calcium signals after both saline administration and dexmedetomidine administration.

Histology

Immunostaining of ventral tegmental area dopamine neurons was performed after all the experiments had been completed. The mice were anesthetized by intraperitoneal injection of pentobarbital (100 mg/kg), and then normal saline was perfused through the heart. After most of the blood was drained, 4% paraformaldehyde was used for fixation. The perfusion was stopped when the limbs became stiff. To further fix the brain tissue, the mice were decapitated, and the heads were soaked in 4% paraformaldehyde at room temperature overnight. The brain tissue was removed the next day and then soaked in phosphate-buffered saline containing 30% sucrose for dehydration for 24 to 48 h. We used a freezing microtome (CM3050S, Leica, Germany) to collect 40-μm-thick coronary brain slices. The slices were washed with phosphate-buffered saline and blocked with a blocking solution (phosphate-buffered saline containing 5% bovine serum albumin and 0.3% Triton X-100 [Acros Organics, Belgium]) for 2 h. After that, primary antibodies (rabbit polyclonal anti–tyrosine hydroxylase; 1:1,000; Catalog no. p21962, Invitrogen, USA) were added to the blocking solution, and slices were incubated for 24 h. The next day, the solution was washed away, and the slices were washed at least three times with phosphate-buffered saline. The secondary antibody used was Alexa Fluor 594 donkey anti-rabbit IgG (1:1,000; Jackson ImmunoResearch, USA) diluted in phosphate-buffered saline and was allowed to coat the brain slices overnight at room temperature. 4',6'-Diamidino-2-phenylindole dihydrochloride staining was used to identify cell bodies, and 10% glycerine was used to mount the slides. Finally, the slices were imaged with a 20× objective on an Olympus VS120 microscope (Olympus, Japan) and a Nikon A1R confocal microscope (Nikon, Japan) using a 40× objective.

The medial prefrontal cortex and nucleus accumbens slices were prepared in the same manner as the ventral tegmental area slices, but immunohistochemistry staining was with 4',6'-diamidino-2-phenylindole dihydrochloride staining only. They were imaged with a 20× objective on an Olympus VS120 microscope and a Nikon A1R confocal microscope using a 40× objective.

Ventral Tegmental Area Slice Preparation

Adult (8 to 12 weeks old) male *DAT-Cre* mice injected with AAV2/9-hsyn-DIO-mCherry in the ventral tegmental area were anesthetized with pentobarbital (100 mg/kg, intraperitoneal injection) and then transcardially perfused with ice-cold oxygenated (95% O_2, 5% CO_2) N-methyl-D-glucamine, a solution that included 93 mM N-methyl-D-glucamine, 93 mM hydrogen chloride, 2.5 mM potassium chloride, 1.25 mM monosodium phosphate, 10 mM magnesium sulphate, 30 mM sodium bicarbonate, 25 mM glucose, 20 mM HEPES, 5 mM sodium ascorbate, 3 mM sodium pyruvate, and 2 mM thiourea. After perfusion, the brain was quickly dissected out and immediately transferred into an ice-cold oxygenated N-methyl-D-glucamine artificial cerebrospinal fluid solution. Then, we sectioned the brain tissue in the coronal plane at a 300-μm thickness in the same buffer using a vibratome (VT1200 S, Leica, Germany). The brain slices containing the ventral tegmental area were incubated in oxygenated N-methyl-D-glucamine artificial cerebrospinal fluid at 32°C for 10 to 15 min and then transferred to a normal oxygenated solution of artificial cerebrospinal fluid (126 mM sodium chloride, 2.5 mM potassium chloride, 1.25 mM monosodium phosphate, 2 mM magnesium sulphate, 10 mM glucose, 26 mM sodium bicarbonate, and 2 mM calcium chloride) at room temperature for 1 h. All chemicals used in the slice preparation were purchased from Sigma-Aldrich (USA).

Downloaded from http://asa2.silverchair.com/anesthesiology/article-pdf/133/2/377/514505/20200800.0-00022.pdf by guest on 13 March 2024

Copyright © 2020, the American Society of Anesthesiologists, Inc. Unauthorized reproduction of this article is prohibited.

In Vitro Electrophysiologic Recordings

Slices were transferred to the recording chamber that was submerged and superfused with artificial cerebrospinal fluid at a rate of 3 ml/min at 28°C. Dopamine-positive neurons were identified with differential interference contrast optics (Olympus BX61WI, Japan). The recording pipettes (3 to 4 MΩ) were prepared with a micropipette puller (P2000, Sutter Instrument, USA). For whole cell recording, the pipettes were filled with artificial cerebrospinal fluid solution containing 133 mM potassium ion gluconate, 18 mM sodium chloride, 0.6 mM EGTA, 10 mM HEPES, 2 mM magnesium–adenosine triphosphate, and 0.3 mM sodium guanosine 5′-triphosphate sodium salt hydrate (pH: 7.2, 280 milliosmole). After the whole cell recording was established, the neurons were held at 0 pA under a current-clamp mode to record spontaneous action potentials. For action potentials evoked by current injections, a current-step protocol (from −50 to +250 pA, with 50 pA increments) was run and repeated. Dexmedetomidine (2 μM) was locally perfused to the recording cell through a drug perfusion system. RS79948 (Tocris Bioscience, United Kingdom; 1 mM) was diluted in fresh artificial cerebrospinal fluid until completely mixed and then transferred to separate graduated reservoirs connected to the chamber (1 to 2 ml/min). During the recordings, baseline levels of spontaneous action potentials were recorded for at least 3 min before the drugs were perfused. To isolate potassium ion currents during the whole cell recordings, tetrodotoxin (1 μM), cadmium chloride (200 μM), 6,7-dinitroquinoxaline-2,3-dione (20 μM), D(-)-2-amino-5-phosphonovaleric acid (20 μM), and picrotoxin (100 μM) were added to the artificial cerebrospinal fluid bath solution to block sodium channels, calcium channels, glutamate receptors, and γ-aminobutyric acid type A receptors, respectively. Potassium ion currents in the ventral tegmental area dopamine cells, in response to depolarizing voltage steps ranging from 0 to +140 mV (in increments of 10 mV), were acquired using a Multiclamp 700B amplifier, and signals were low-pass filtered at 3 kHz and digitized at 10 kHz (DigiData 1550, Molecular Devices, USA). The physiologic data were analyzed using Clampfit 10 software (Molecular Devices, USA) and Mini Analysis Program (Synaptosoft, USA).

EEG Recording and Analysis

We implanted EEG electrodes following previously described procedures.[26] Briefly, after being deeply anesthetized by intraperitoneal injections of pentobarbital (50 mg/kg), the mice were placed on the stereoscopic positioning instrument and were kept warm (37°C) with an electric heating pad. Three holes were drilled with a carbide bit: one over the left frontal cortical area (1 mm anterior to bregma, 1.5 mm lateral to midline), another over the parietal area (1 mm anterior to lambda, 1.5 mm lateral to midline) of the right hemisphere, and a third over the parietal area (1 mm anterior to lambda, 1.5 mm lateral to midline) of the left hemisphere. Then, three electrodes were implanted in the holes and fixed in place with dental cement. After the dental cement was completely dried, the mice were removed from the stereoscopic positioning instrument and placed on an electric blanket. When the mice fully recovered, they were returned to their home cage. EEG recordings were conducted 14 days after surgery. EEG data were digitized at 1 kHz by the PowerLab and LabChart system (AD Instruments, New Zealand), low-pass filtered at 0.3 Hz, and high-pass filtered at 50 Hz. The power spectrum between 0.1 and 30 Hz was transformed using the "mtspecgramc" function in the MATLAB signal processing toolbox chronux_2_12 (MathWorks, USA).[27] The EEG changes between frequency bands were used to estimate the sedation states: delta (δ: 0.5 to 4 Hz), theta (θ: 4 to 7 Hz), alpha (α: 8 to 15 Hz), and beta (β: 16 to 30 Hz).[28]

Chemogenetic Activation or Inhibition of Ventral Tegmental Area Dopamine Neurons

Before the testing day, the mice were handled for 30 min on each of 5 days and adapted to having the EEG device connected to their head for 30 min in the testing room on each of 3 days. They were put into the testing room 1 h before the behavioral test for acclimation. The mice were then intraperitoneally injected with clozapine N-oxide (1 mg/kg). After 30 min, they were injected with dexmedetomidine (40 μg/kg), and EEG was immediately recorded for at least 1 h.

Statistical Analysis

We randomized animals to the different treatment groups using the random number table method, and mice in each group were tested in ascending order. We also blinded the experimenters to the drug treatment to reduce selection and observation bias. None of the variables had missing data. Outliers were evaluated, and there were no outliers in our data. Graph Pad Prism 7.0 (GraphPad Software, USA), MATLAB R2018b, and IBM SPSS Statistics 19 software (IBM, USA) were used for statistical evaluation. Quantile–quantile plots were used to assess whether the sample conformed to a normal distribution. A paired Student's *t* test was used for the fiber recording and patch-clamp recording. Two-way repeated-measures ANOVA with Bonferroni posttest was used for the patch-clamp recording and EEG recording. The Kruskal–Wallis one-way ANOVA test was used to detect the difference in EEG waveform distributions among the different groups over time. No statistical methods were used to predetermine the sample size. All tests were two-tailed, and $P < 0.05$ was considered significant in all tests. Data were accurately reported according to the original data to avoid false precision. Unless otherwise indicated, values were reported as the mean ± SD.

Downloaded from http://asa2.silverchair.com/anesthesiology/article-pdf/133/2/377/514505/20200800.0-00022.pdf by guest on 13 March 2024

Copyright © 2020, the American Society of Anesthesiologists, Inc. Unauthorized reproduction of this article is prohibited.

Results

Dexmedetomidine Activated Ventral Tegmental Area Dopamine Neurons

To study the effect of systemic administration of dexmedetomidine on ventral tegmental area dopamine neurons, we injected the Cre-dependent AAV-EF1α-DIO-GCaMP6m virus into the ventral tegmental area of *DAT-Cre* mice and used fiber photometry to record changes in Ca^{2+} signals *in vivo* (fig. 1A). The virus was expressed as in figure 1B, and the calcium indicator GCaMP6m was expressed in dopamine neurons (fig. 1C). In freely moving mice, the GCaMP6m signals ranged from –20 to 60% (ΔF/F), and the control GFP signal showed little fluctuation, indicating that the fluctuations were caused by Ca^{2+} binding (Supplemental Digital Content, fig. S1, http://links.lww.com/ALN/C383).[25] In response to peer review, additional dose-response experiments with dexmedetomidine were performed. The results showed that after intraperitoneal injection of saline or dexmedetomidine (10 μg/kg), the Ca^{2+} signals exhibited almost no change (fig. 1D). Statistical analysis showed that the average Ca^{2+} signals after administration of dexmedetomidine were approximately equal to those after administration of saline (dexmedetomidine, 0.460 [–1.283; 1.734], median [25%; 75%] *vs.* saline, –0.591 [–1.153; 0.640], normalized data, $P = 0.751$; n = 6 mice; fig. 1E). However, after intraperitoneal injection of dexmedetomidine (40, 100, and 400 μg/kg), the Ca^{2+} signals significantly increased (fig. 1, F, H, and J). Statistical analyses showed that the average Ca^{2+} signals after administration of dexmedetomidine were significantly higher than those after administration of saline (dexmedetomidine, 16.917 [14.882; 21.748], median [25%; 75%] *vs.* saline, –0.745 [–1.547; 0.359], normalized data, $P = 0.001$; n = 6 mice; fig. 1G; dexmedetomidine, 17.383 [12.325; 20.994], median [25%; 75%] *vs.* saline, –0.400 [–1.821; 0.048], normalized data, $P < 0.0001$; n = 6 mice; fig. 1I; dexmedetomidine, 21.738 [20.403; 27.561], median [25%; 75%] *vs.* saline, 0.087 [–1.722; 0.544], normalized data, $P < 0.0001$; n = 6 mice; fig. 1K).

Dexmedetomidine Increased Dopamine Neurotransmitter in the Medial Prefrontal Cortex and Nucleus Accumbens

To investigate whether dexmedetomidine had an influence on the change in dopamine neurotransmitter in the related forebrain projection areas of ventral tegmental area dopamine neurons, we injected AAV-hsyn-DA1m virus into the medial prefrontal cortex and nucleus accumbens of C57BL/6J mice.[29] Virus expression and fiber position are shown in figure 2, A and B, and figure 3, A and B. DA1m signals ranged from –5 to 15% (ΔF/F) when the test mouse was freely moving. There was almost no change in the DA1m-mut signals in the control group (Supplemental Digital Content, fig. S1, http://links.lww.com/ALN/C383). This implied that the signal fluctuations were caused by changes in dopamine neurotransmitter.[29] In response to peer review, additional dose-response experiments for dexmedetomidine were performed. The results showed that after the injection of normal saline and dexmedetomidine (10 μg/kg), the DA1m signals exhibited almost no change (figs. 2C and 3C). Statistical analyses showed that the average DA1m signals after administration of dexmedetomidine were approximately equal to those after administration of saline (dexmedetomidine, –0.708 [–1.118; 0.376], median [25%; 75%] *vs.* saline, 0.093 [–0.003; 0.249], normalized data, $P = 0.241$; n = 6 mice; fig. 2D; dexmedetomidine, 0.714 [–0.430; 1.382], median [25%; 75%] *vs.* saline, 0.096 [0.029; 0.396], normalized data, $P = 0.326$; n = 6 mice; fig. 3D). However, after the injection of dexmedetomidine (40, 100, and 400 μg/kg), the DA1m signals markedly increased (figs. 2E, 2G, 2I, 3E, 3G, and 3I). Statistical analyses showed that the DA1m signals in the medial prefrontal cortex and nucleus accumbens were significantly increased after systemic administration of dexmedetomidine (dexmedetomidine, 10.815 [9.713; 15.104], median [25%; 75%] *vs.* saline, –0.498 [–0.664; -0.355], normalized data, $P = 0.001$; n = 6 mice; fig. 2F; dexmedetomidine, 7.521 [5.615; 12.809], median [25%; 75%] *vs.* saline, –0.274 [–0.428; –0.136], normalized data, $P = 0.003$; n = 6 mice; fig. 2H; dexmedetomidine, 15.312 [12.330; 16.337], median [25%; 75%] *vs.* saline, –0.181 [–0.878; 0.016], normalized data, $P < 0.0001$; n = 6 mice; fig. 2J; dexmedetomidine, 8.543 [7.135; 11.828], median [25%; 75%] *vs.* saline, –0.329 [–1.220; –0.047], normalized data, $P = 0.001$; n = 6 mice; fig. 3F; dexmedetomidine, 11.309 [10.557; 14.164], median [25%; 75%] *vs.* saline, –0.706 [–1.226; –0.251], normalized data, $P < 0.0001$; n = 6 mice; fig. 3H; dexmedetomidine, 11.296 [8.199; 12.092], median [25%; 75%] *vs.* saline, –0.339 [–0.561; 0.089], normalized data, $P = 0.002$; n = 6 mice; fig. 3J).

Patch-clamp Recording Revealed that Dexmedetomidine Activated Ventral Tegmental Area Dopamine Neurons

To further investigate the mechanism by which dexmedetomidine activated ventral tegmental area dopamine neurons, we used slice electrophysiology technology. Whole cell recording showed that ventral tegmental area dopamine neurons were intrinsically active and tonically fired. Interestingly, the firing frequency clearly increased after dexmedetomidine perfusion (fig. 4A). There was a statistically significant difference in the firing frequencies before and after dexmedetomidine perfusion (before: 5.046 ± 5.057 Hz and after: 8.600 ± 7.387 Hz, $P = 0.031$; n = 11 neurons; fig. 4B). The current-injected firing also showed that after dexmedetomidine perfusion, the peak density visibly increased compared to that with artificial cerebrospinal fluid perfusion (fig. 4C). Statistical analyses revealed that as the injection current increased from –50 pA to 250 pA, the

Downloaded from http://asa2.silverchair.com/anesthesiology/article-pdf/133/2/377/514505/20200800.0-00022.pdf by guest on 13 March 2024

Copyright © 2020, the American Society of Anesthesiologists, Inc. Unauthorized reproduction of this article is prohibited.

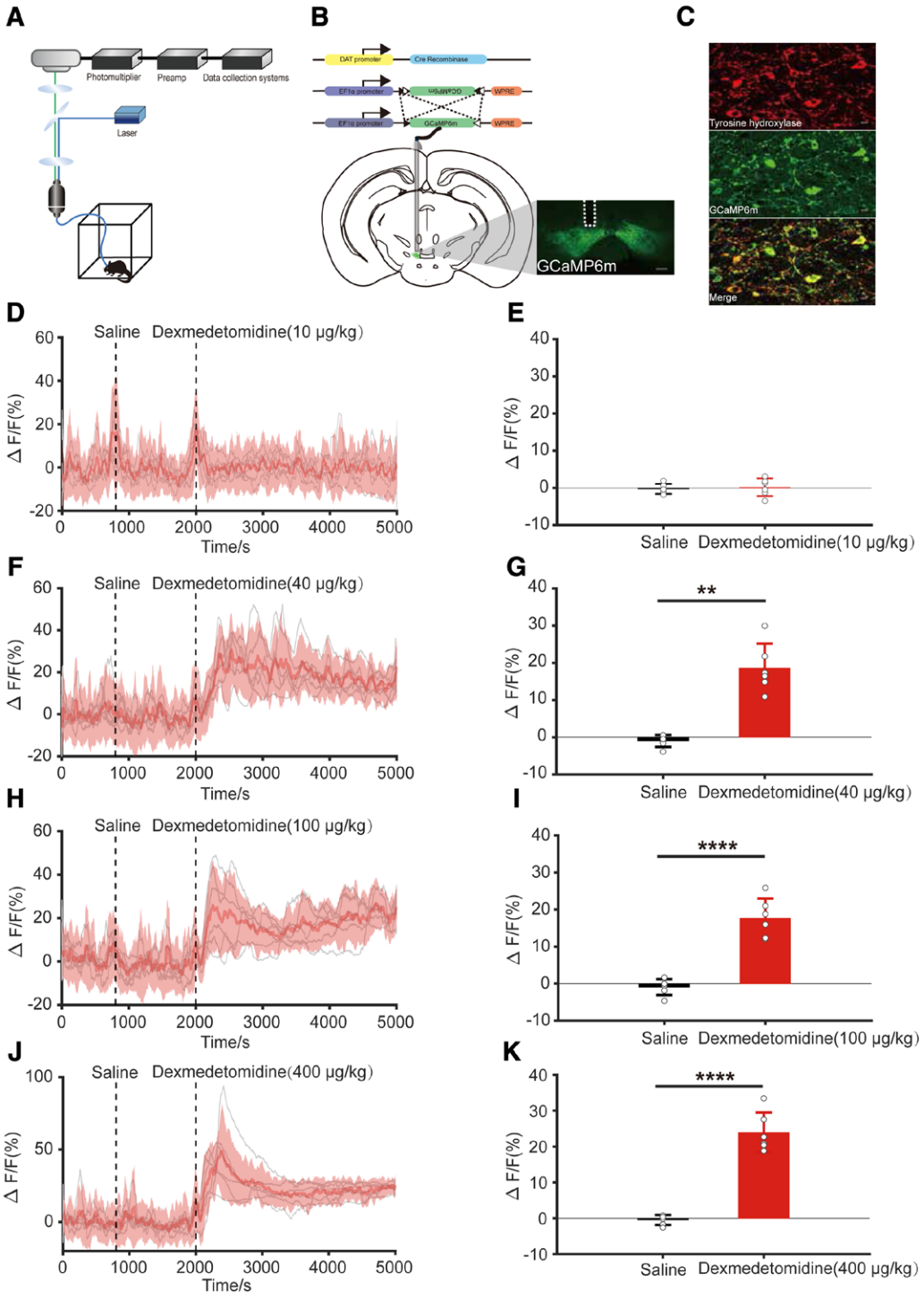

Fig. 1. Systemic administration of dexmedetomidine activated ventral tegmental area dopamine neurons. (*A*) Schematic of fiber recording. (*B*) Schematic of fiber implantation above ventral tegmental area dopamine neurons expressing GCaMP6m. Scale bar: 200 μm. (*C*) Tyrosine hydroxylase immunopositive neurons and GCaMP6m-expressing neurons in the ventral tegmental area of a *DAT-Cre* mouse. Scale bar: 20 μm. (*D, F, H, and J*) GCaMP6m signals from ventral tegmental area dopamine neurons aligned to the moment of the administration of saline and dexmedetomidine. The data shown in *gray lines* represent the signals from each mouse. Mean values are shown as a *red line*, and the SD interval is *shaded in red* (n = 6 mice). (*E, G, I, and K*) Quantification of the changes in GCaMP6m signals after administration of saline and dexmedetomidine. Error bars indicate the SD. Paired Student's *t* test: $^{**}P < 0.01$, $^{****}P < 0.0001$; n = 6 mice. Details of statistical analysis are presented in Supplemental Digital Content, table S2 (http://links.lww.com/ALN/C384).

Downloaded from http://asa2.silverchair.com/anesthesiology/article-pdf/133/2/377/514505/20200800.0-00022.pdf by guest on 13 March 2024

Copyright © 2020, the American Society of Anesthesiologists, Inc. Unauthorized reproduction of this article is prohibited.

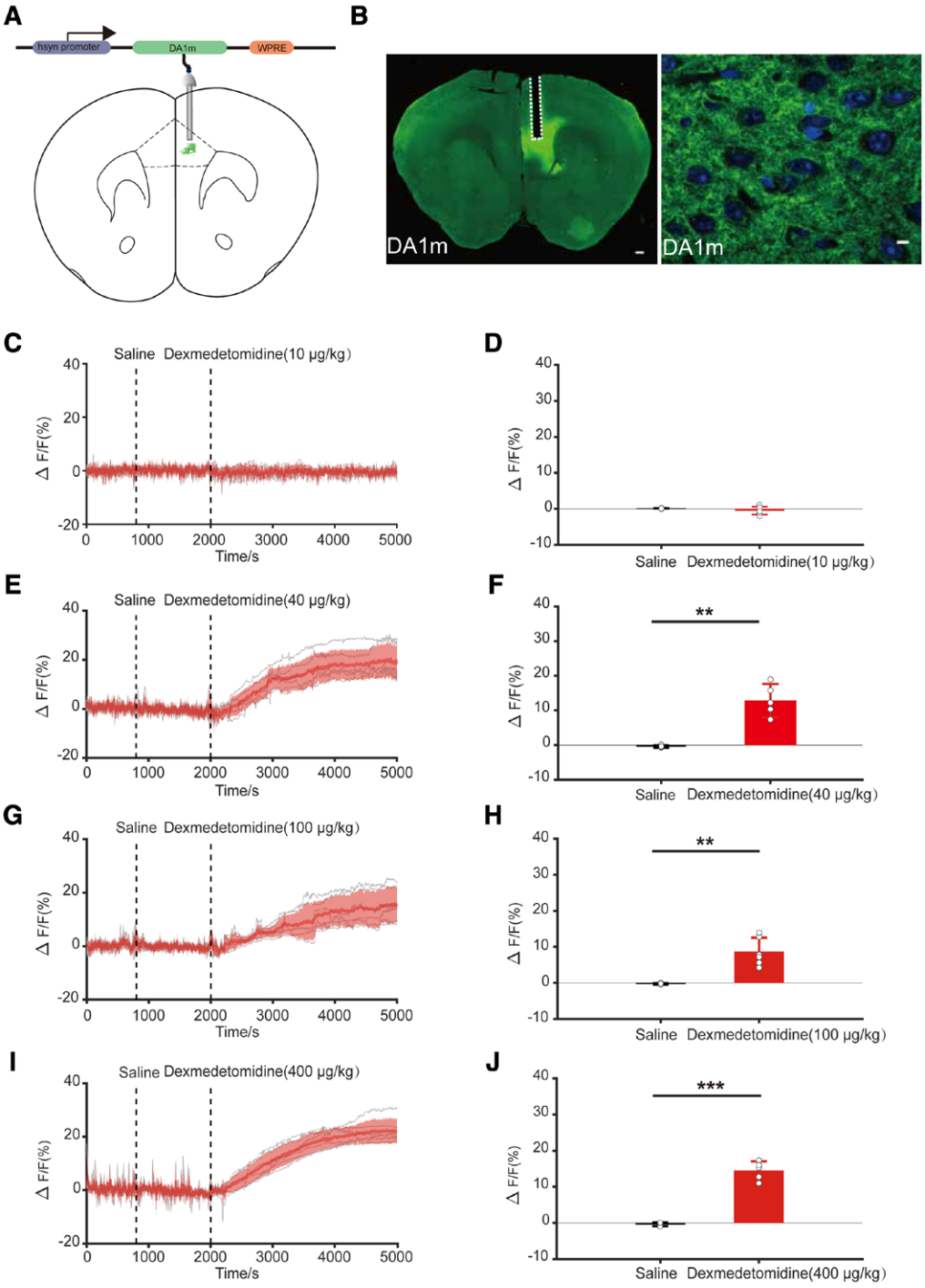

Fig. 2. Systemic administration of dexmedetomidine increased the concentrations of dopamine neurotransmitter in the medial prefrontal cortex. (*A*) Schematic of stereotactic virus injection into the medial prefrontal cortex of C57BL/6J mice. (*B*) Schematic of fiber implantation above DA1m-marked medial prefrontal cortex neurons. *Left*: Scale bar: 200 μm. *Right*: Scale bar: 15 μm. (*C, E, G, and I*) DA1m signals from medial prefrontal cortex neurons aligned to the moment of the administration of saline and dexmedetomidine. The data shown in *gray lines* represent the signals of each mouse. Mean values are shown as a *red line*, and the SD interval is *shaded in red* (n = 6 mice). (*D, F, H, and J*) Quantification of the changes in DA1m signals after administration of saline and dexmedetomidine. Error bars indicate the SD. Paired Student's *t* test: $^{**}P < 0.01$, $^{***}P < 0.001$; n = 6 mice. DA1m, G protein-coupled receptor-activation-based dopamine sensor; DA1m-mut, mutant G protein-coupled receptor-activation-based dopamine sensor. Details of statistical analysis are presented in Supplemental Digital Content, table S2 (http://links.lww.com/ALN/C384).

Downloaded from http://asa2.silverchair.com/anesthesiology/article-pdf/133/2/377/514505/20200800.0-00022.pdf by guest on 13 March 2024

Copyright © 2020, the American Society of Anesthesiologists, Inc. Unauthorized reproduction of this article is prohibited.

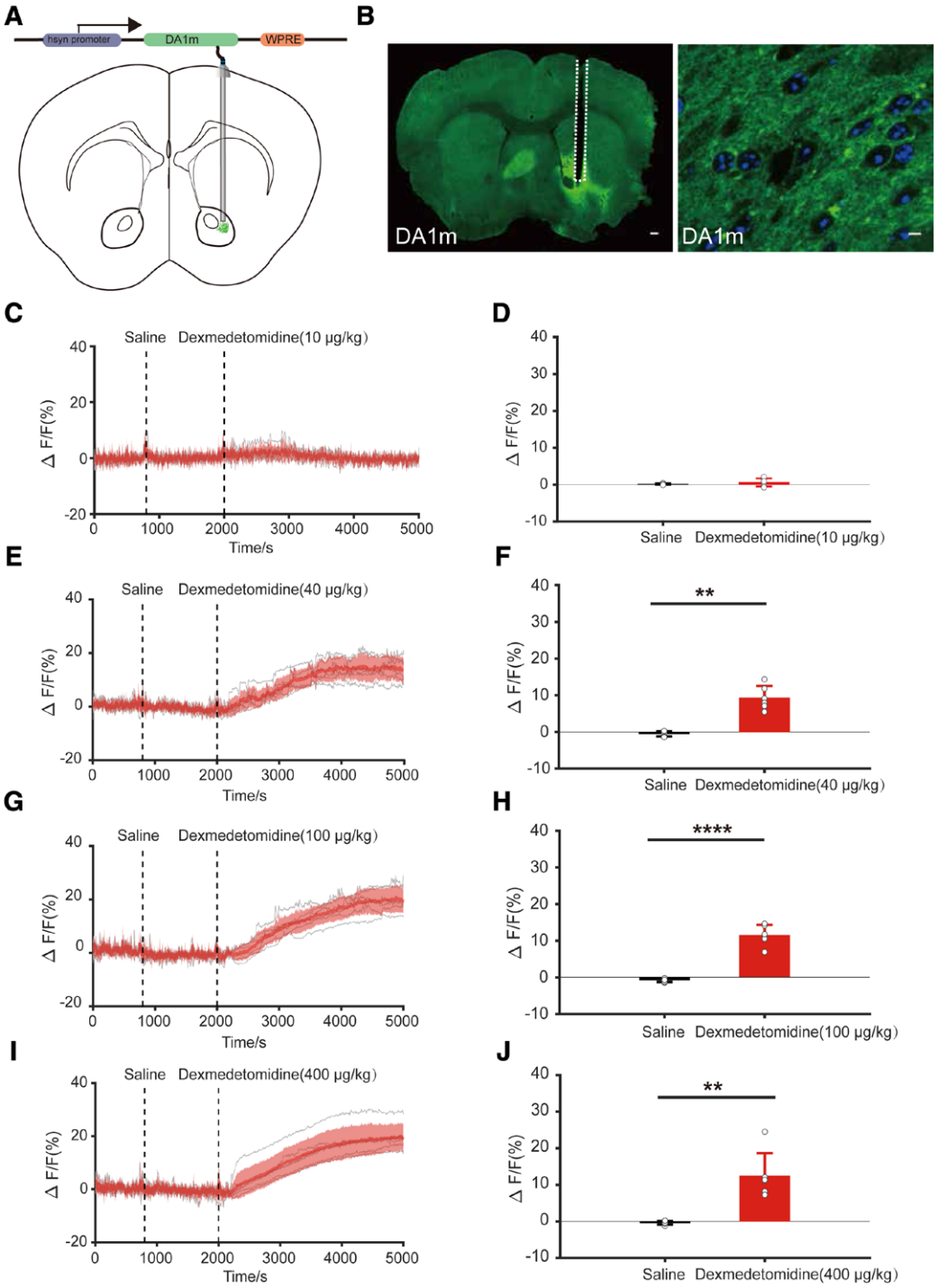

Fig. 3. Systemic administration of dexmedetomidine increased the concentrations of dopamine neurotransmitter in the nucleus accumbens. (*A*) Schematic of stereotactic virus injection into the nucleus accumbens of C57BL/6J mice. (*B*) Schematic of fiber implantation above DA1m-marked nucleus accumbens neurons. *Left*: Scale bar: 200 μm. *Right*: Scale bar: 15 μm. (*C, E, G, and I*) DA1m signals from nucleus accumbens neurons aligned to the moment of the administration of saline and dexmedetomidine. The data shown in *gray lines* represent the signals of each mouse. Mean values are shown as a *red line*, and the SD interval is *shaded in red* (n = 6 mice). (*D, F, H, and J*) Quantification of the changes in DA1m signals after administration of saline and dexmedetomidine. Error bars indicate the SD. Paired Student's *t* test: $^{**}P < 0.01$, $^{****}P < 0.0001$; n = 6 mice. DA1m, G protein-coupled receptor-activation-based dopamine sensor; DA1m-mut, mutant G protein-coupled receptor-activation-based dopamine sensor. Details of statistical analysis are presented in Supplemental Digital Content, table S2 (http://links.lww.com/ALN/C384).

Downloaded from http://asa2.silverchair.com/anesthesiology/article-pdf/133/2/377/514505/20200800.0-00022.pdf by guest on 13 March 2024

Copyright © 2020, the American Society of Anesthesiologists, Inc. Unauthorized reproduction of this article is prohibited.

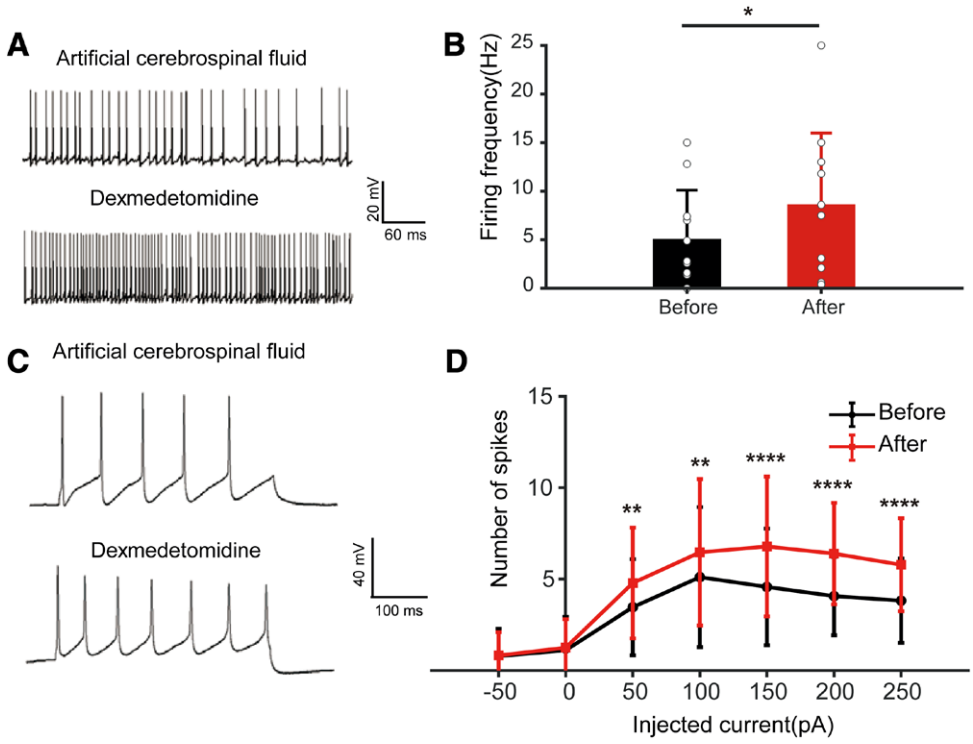

Fig. 4. Dexmedetomidine activated ventral tegmental area dopamine neurons in an acute brain slice preparation. (*A*) Whole cell patch-clamp recording showed that intrinsic neuronal firing after dexmedetomidine (2 μM) perfusion was faster than after perfusion with artificial cerebrospinal fluid. (*B*) Statistical analysis showed that after dexmedetomidine perfusion, the firing frequency was significantly increased over the rate after artificial cerebrospinal fluid perfusion. Error bars indicate the SD (paired Student's *t* test, $*P < 0.05$, n = 11 neurons). (*C*) Measurement of current-injected firing showed that after perfusion with dexmedetomidine, the number of spikes was greater than after perfusion with artificial cerebrospinal fluid. (*D*) Statistics showed that as the injection current increased (from –50 pA to 250 pA), the number of spikes was significantly increased over the number seen with artificial cerebrospinal fluid perfusion, especially at 150 pA and 200 pA. Two-way repeated measures ANOVA with Bonferroni posttest: $*P < 0.05$, $**P < 0.01$, $****P < 0.0001$; n = 28 neurons. Details of statistical analysis are presented in Supplemental Digital Content, table S2 (http://links.lww.com/ALN/C384).

number of spikes was significantly higher after dexmedetomidine perfusion than after artificial cerebrospinal fluid perfusion, especially at 150 pA and 200 pA ($F[1, 27]$, $P < 0.0001$; n = 28 neurons; fig. 4D).

Dexmedetomidine Inhibited Potassium Ion Conductance by Activating α2 Adrenoceptors

In response to peer review, additional experiments providing a more in-depth electrophysiologic characterization for mechanistic insights were performed. Given that dexmedetomidine is a highly selective α2 adrenoceptor agonist, we used a selective α2 adrenoceptor antagonist (RS79948)[30,31] to explore whether it can antagonize the effect of dexmedetomidine activation of ventral tegmental area neurons. The results showed that the intrinsic neuronal firing after dexmedetomidine (2 μM) perfusion was similar to artificial cerebrospinal fluid in the presence of RS79948 (1 mM; fig. 5A). Statistical analysis indicated that the firing frequency showed no difference between artificial cerebrospinal fluid and dexmedetomidine in the presence of RS79948 (before: 3.970 ± 1.927 Hz and after: 3.810 ± 1.849 Hz, $P = 0.100$; n = 10 neurons; fig. 5B). Koo *et al.*[32] found that morphine increased the excitability of ventral tegmental area dopamine neurons by inhibiting potassium ion currents. We speculated that dexmedetomidine activation of ventral tegmental area dopamine neurons was also related to this mechanism. In voltage-clamp mode, the potassium ion current was significantly suppressed after perfusion with dexmedetomidine compared with artificial cerebrospinal fluid (fig. 5C). The peaks of the potassium ion currents in the ventral tegmental area dopamine neurons were reduced by dexmedetomidine compared with artificial cerebrospinal fluid ($F[1, 14] = 16.09$, $P = 0.001$; n = 15 neurons; fig. 5D). However, the potassium ion currents showed almost no difference between artificial cerebrospinal fluid and dexmedetomidine perfusion in the presence of RS79948 (fig. 5E). The peaks of the potassium ion currents in the ventral tegmental area dopamine neurons also showed no statistically significant difference between artificial

Downloaded from http://asa2.silverchair.com/anesthesiology/article-pdf/133/2/377/514505/20200800.0-00022.pdf by guest on 13 March 2024

Copyright © 2020, the American Society of Anesthesiologists, Inc. Unauthorized reproduction of this article is prohibited.

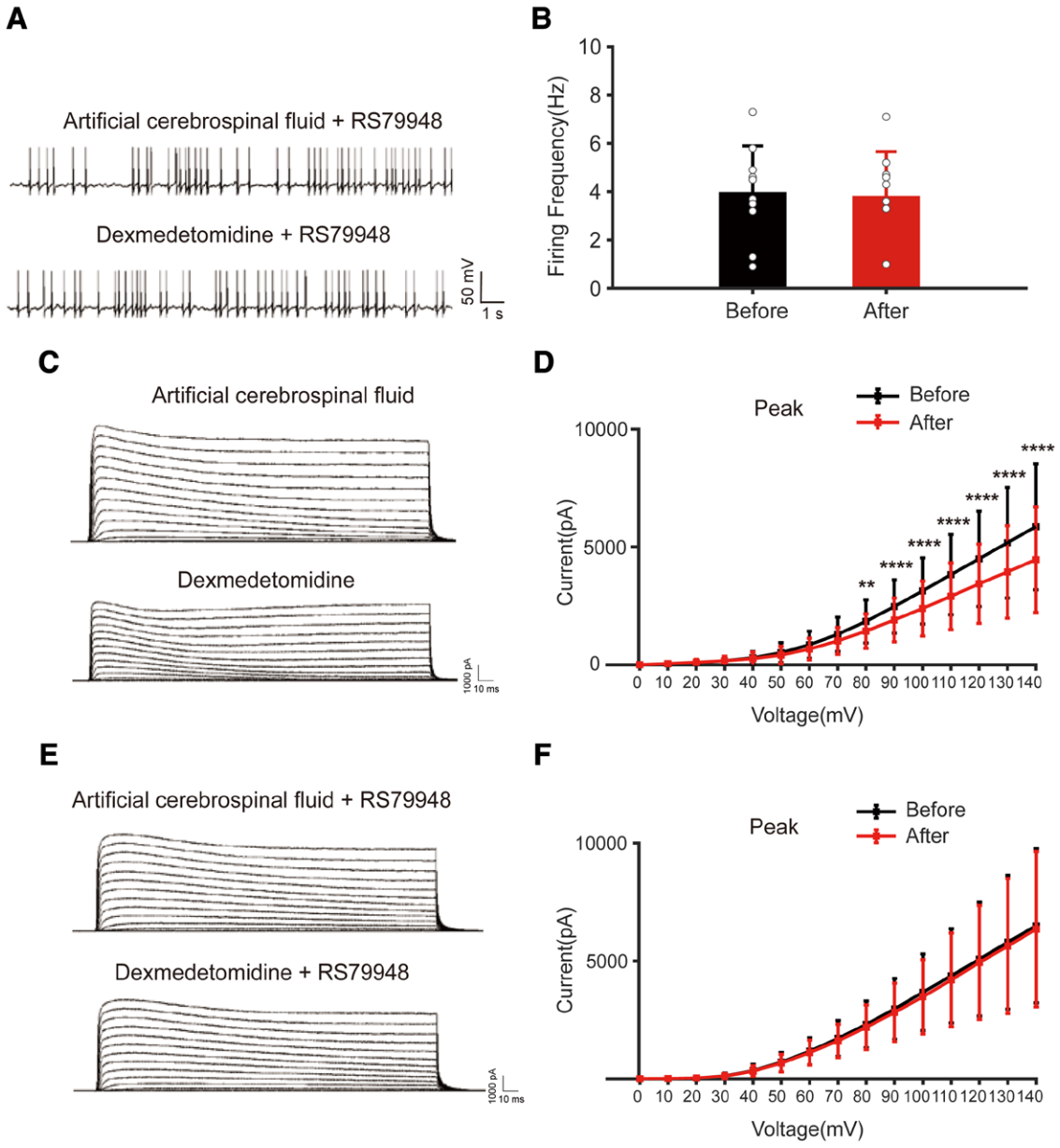

Fig. 5. Dexmedetomidine inhibits potassium ion conductance by activating α2 adrenoceptors. (*A*) Whole cell patch-clamp recording shows that the intrinsic neuronal firing after dexmedetomidine (2 μM) perfusion was similar to that with artificial cerebrospinal fluid in the presence of RS79948 (1 mM). (*B*) Statistical analysis showed that the firing frequency was not different between artificial cerebrospinal fluid and dexmedetomidine perfusion in the presence of RS79948 (paired Student's *t* test, $P > 0.05$; n = 10 neurons). (*C*) Sample traces of potassium ion conductance recorded in brain slices after artificial cerebrospinal fluid and dexmedetomidine perfusion. (*D*) Dexmedetomidine significantly decreased potassium ion currents in ventral tegmental area dopamine neurons (two-way repeated measures ANOVA with Bonferroni posttest, $P < 0.0001$; n = 15 neurons). (*E*) Sample traces of potassium ion conductance recorded in brain slices after artificial cerebrospinal fluid and dexmedetomidine perfusion in the presence of RS79948. (*F*) Statistical analysis showed that the potassium ion currents showed no difference between artificial cerebrospinal fluid and dexmedetomidine perfusion in the presence of RS79948 (two-way repeated measures ANOVA with Bonferroni posttest, $P > 0.05$; n = 10 neurons). Two-way repeated measures ANOVA with Bonferroni posttest: $^{**}P < 0.01$, $^{****}P < 0.0001$. Details of statistical analysis are presented in Supplemental Digital Content, table S2 (http://links.lww.com/ALN/C384).

Downloaded from http://asa2.silverchair.com/anesthesiology/article-pdf/133/2/377/514505/20200800.0-00022.pdf by guest on 13 March 2024

Copyright © 2020, the American Society of Anesthesiologists, Inc. Unauthorized reproduction of this article is prohibited.

cerebrospinal fluid and dexmedetomidine perfusion in the presence of RS79948 (F[1, 9] = 4.019, P = 0.076; n = 10 neurons; fig. 5F).

The Sedative Effect of Dexmedetomidine Was Deepened or Attenuated after Inhibiting or Activating, Respectively, Ventral Tegmental Area Dopamine Neurons

We used chemogenetics to inhibit ventral tegmental area dopamine neurons to test for exacerbation of dexmedetomidine sedation. In response to peer review, additional experiments with chemogenetic activation of ventral tegmental area neurons to test for resistance to dexmedetomidine sedation were also performed. The experimental design is shown in figure 6A. We bilaterally infused Cre-dependent AAV-DIO-hM4Di-mCherry, AAV-DIO-hM3Dq-mCherry, and AAV-DIO-mCherry vectors into the ventral tegmental area of *DAT-Cre* mice (fig. 6B). After administration of clozapine N-oxide, ventral tegmental area dopamine neurons in the brain slice preparations were significantly inhibited or activated (fig. 6, C and D). During the test, all mice underwent systemic delivery of clozapine N-oxide (1 mg/kg, intraperitoneally) 30 min before systemic delivery of dexmedetomidine (40 μg/kg, intraperitoneally) and EEG recording. The dose of dexmedetomidine is sufficient to induce slow-wave sedation in mice.[4,33] The EEG waveform pattern and spectrum showed that the power of low-frequency waves was increased in the hM4Di group and reduced in the hM3Dq group in comparison to the mCherry group (fig. 6E). The percentages of delta waves per minute among the mCherry, hM3Dq, and hM4Di groups were significantly different (F[2, 33] = 8.016, P = 0.002, n = 12 mice, fig. 6F; P < 0.0001, n = 12 mice, fig. 6G). The percentages of delta waves per minute between the mCherry and hM3Dq groups were significantly different (F[1, 22] = 6.974, P = 0.015, n = 12 mice). There were no significant differences between the mCherry and hM4Di groups (F[1, 22]=1.294, P = 0.268, n = 12 mice). However, there was a trend that the percentages of delta waves per minute in the hM4Di group were greater than those in the mCherry group (fig. 6, F and G). The percentages of theta waves per minute among the mCherry, hM3Dq, and hM4Di groups were also significantly different (F[2, 33] = 22.8, P < 0.0001, n = 12 mice, fig. 6H; P < 0.0001, n = 12 mice, fig. 6I). The percentages of theta waves per minute between the mCherry and hM3Dq groups were significantly different (F[1, 22]=14.82, P = 0.001; n = 12 mice). The percentages of theta waves per minute between the mCherry and hM4Di groups were also significantly different (F[1, 22]=7.348, P = 0.013; n = 12 mice).

Discussion

The purpose of this study was to examine the mechanisms underlying arousability properties of dexmedetomidine using *in vivo* Ca^{2+} measurement, *in vitro* slice recording, chemogenetics, and EEG recording. The results showed that ventral tegmental area dopamine neurons were activated and dopamine neurotransmitters were increased in the targeted forebrain regions after systemic administration of dexmedetomidine. Patch-clamp recording showed that dexmedetomidine activated ventral tegmental area dopamine neurons through the α2 adrenoceptors and inhibited potassium ion conductance by activating the α2 adrenoceptors. EEG recordings confirmed that after the inhibition of ventral tegmental area dopamine neurons, the depth of sedation with dexmedetomidine was deepened. Conversely, after activation of ventral tegmental area dopamine neurons, the depth of sedation with dexmedetomidine was attenuated.

Patch-clamp recording revealed that dexmedetomidine inhibited potassium ion conductance and activated ventral tegmental area dopamine neurons. However, after perfusion with an α2 adrenoreceptor antagonist (RS79948), there were no statistically significant differences in the excitability and potassium ion conductance of ventral tegmental area dopamine neurons. Koo *et al.*[32] found that morphine increased the excitability of ventral tegmental area dopamine neurons by inhibiting potassium ion conductance. Therefore, dexmedetomidine inhibited potassium ion conductance in the ventral tegmental area dopamine neurons by activating α2 adrenoceptors on the ventral tegmental area dopamine neurons, resulting in increased excitability of ventral tegmental area dopamine neurons. This led to an increase in dopamine neurotransmitter in the targeted forebrain regions, *i.e.*, the nucleus accumbens and medial prefrontal cortex.

Dexmedetomidine is commonly used as a sedative drug. It has primarily been thought to target the norepinephrine system. Many studies have shown that dexmedetomidine acts on α2 adrenoceptors on locus coeruleus norepinephrine neurons and then hyperpolarizes cell membranes through a Gi-coupling mechanism. The release of the excitatory neurotransmitter norepinephrine is subsequently decreased throughout the brain, which eventually leads to sedation.[3] Previous studies have also shown that ventral tegmental area dopamine neurons are associated with sleep and arousal.[16–21,34] However, the relationship between dexmedetomidine and activity in the ventral tegmental area dopamine system has remained unknown. Our results showed that dexmedetomidine activated ventral tegmental area dopamine neurons and increased dopamine concentrations in the targeted forebrain regions. After the inhibition of ventral tegmental area dopamine neurons, sedation with dexmedetomidine deepened. This is consistent with previous results showing that inhibiting ventral tegmental area dopamine neurons promoted sleep in mice.[18] Conversely, after activation of ventral tegmental area dopamine neurons, sedation with dexmedetomidine was attenuated. This is consistent with previous results showing that activating

Downloaded from http://asa2.silverchair.com/anesthesiology/article-pdf/133/2/377/514505/20200800.0-00022.pdf by guest on 13 March 2024

Copyright © 2020, the American Society of Anesthesiologists, Inc. Unauthorized reproduction of this article is prohibited.

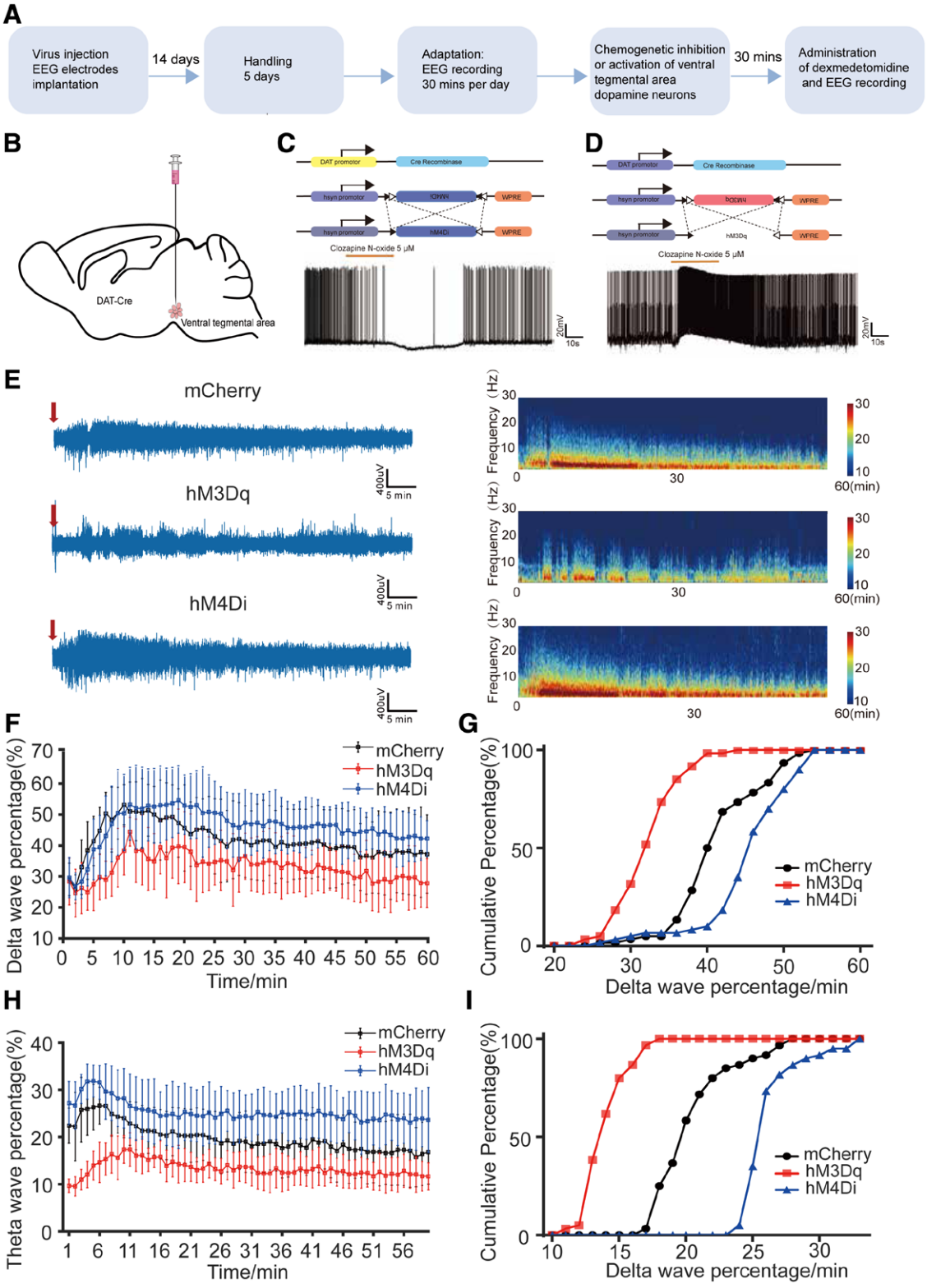

Fig. 6. (*Continued*)

Downloaded from http://asa2.silverchair.com/anesthesiology/article-pdf/133/2/377/514505/20200800.0-00022.pdf by guest on 13 March 2024

Copyright © 2020, the American Society of Anesthesiologists, Inc. Unauthorized reproduction of this article is prohibited.

Fig. 6. (Continued). Inhibition or activation of ventral tegmental area dopamine neurons deepened or attenuated respectively the sedation depth with dexmedetomidine. (*A*) The experimental procedure for chemogenetic inhibition or activation of ventral tegmental area dopamine neurons and electroencephalography (EEG) recordings. (*B*) Schematic of stereotactic virus injection into the ventral tegmental area of *DAT-Cre* mice. (*C and D*) A representative trace of clozapine N-oxide (5 μM) application-evoked hyperpolarization or depolarization potentials during whole cell patch-clamp recordings. (*E*) Representative power spectral density of EEG data. *Warm colors* (*e.g.*, *red*) represent higher power at a given frequency, while *cool colors* (*e.g.*, *blue*) represent lower power. The *red arrow* indicates the moment of administration of dexmedetomidine (40 μg/kg). (*F*) After administration of dexmedetomidine, the delta wave percentage per minute was significantly different among the mCherry, hM3Dq, and hM4Di groups (two-way repeated measures ANOVA with Bonferroni posttest, $P < 0.01$; n = 12 mice). (*G*) Cumulative probability of delta wave percentage per minute (Kruskal–Wallis one-way ANOVA, $P < 0.0001$; n = 12 mice). (*H*) After administration of dexmedetomidine, theta wave percentage per minute was significantly different among the mCherry, hM3Dq, and hM4Di groups (two-way repeated measures ANOVA with Bonferroni posttest, $P < 0.0001$; n = 12 mice). (*I*) Cumulative probability of theta wave percentage per minute (Kruskal–Wallis one-way ANOVA, $P < 0.0001$; n = 12 mice). hM3Dq, Gq-coupled human M3 muscarinic receptor; hM4Di, Gi-coupled human M4 muscarinic receptor. Details of statistical analysis are presented in Supplemental Digital Content, table S2 (http://links.lww.com/ALN/C384).

ventral tegmental area dopamine neurons promoted awakening in mice.[17,18] We conclude that dexmedetomidine activates ventral tegmental area dopamine neurons (arousal-promoting neurons), which can lower the threshold of arousal during dexmedetomidine sedation. This may be involved in the unique sedative feature of dexmedetomidine that enables patients to be easily arousable (fig. 7).

Some studies have focused on changes in dopamine concentrations in the nucleus accumbens or medial prefrontal cortex after systemic administration of dexmedetomidine. Whittington *et al.*[23] and Whittington and Virág[24] found that dexmedetomidine decreased the concentrations of accumbal dopamine in rats, and this effect was partly mediated *via* the locus coeruleus. Ihalainen and Tanila[22,35] also showed the same results in the medial prefrontal cortex and nucleus accumbens of mice. However, our findings are not consistent with these studies. One reason for this may be that we used different animal strains. Another reason may be that we used different experimental methods. Previous studies have used microdialysis to measure changes in dopamine neurotransmitter concentrations in the medial prefrontal cortex and nucleus accumbens. However, there are several evident disadvantages of the microdialysis method. The temporal resolution of microdialysis is considerably slower than many dynamic processes in the central nervous system.[36] In addition, the probe (>250 μm in diameter) used

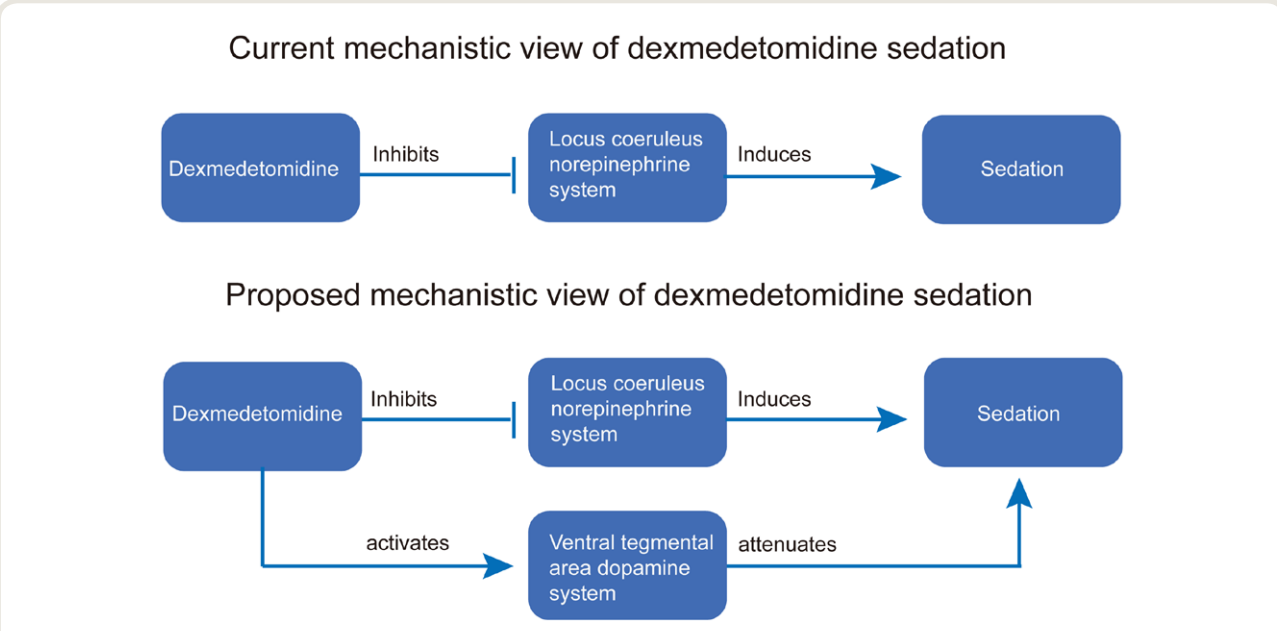

Fig. 7. Schematic diagram of dexmedetomidine-induced sedation. It has been believed that the sedation of dexmedetomidine results from the inhibition of locus coeruleus norepinephrine neurons and a consequent decrease in norepinephrine transmission throughout the whole brain. Our research found that dexmedetomidine activates the ventral tegmental area dopamine system, which has an arousal promotion effect. This may lower the threshold of arousal during dexmedetomidine sedation and may be involved in the unique sedative features of dexmedetomidine that enable patients to be easily arousable.

Downloaded from http://asa2.silverchair.com/anesthesiology/article-pdf/133/2/377/514505/20200800.0-00022.pdf by guest on 13 March 2024

Copyright © 2020, the American Society of Anesthesiologists, Inc. Unauthorized reproduction of this article is prohibited.

in microdialysis can induce extensive tissue damage with inflammation, gliosis, and swollen axons.[37] Borland *et al.*[38] found that after acute implantation, the release of dopamine was strongly inhibited in the vicinity of the probe, as the dialysis probe was surrounded by scar tissue soon after implantation, and therefore, the microdialysis method might represent a neuropathological rather than a neurophysiological condition. However, we used fiber photometry recording technology to confirm that dexmedetomidine activated ventral tegmental area dopamine neurons and increased forebrain dopamine neurotransmitters. The optical fiber was implanted above the brain area and would not cause damage to the brain area of interest. We also confirmed that dexmedetomidine activated ventral tegmental area dopamine neurons *in vivo* and *in vitro* and how dexmedetomidine activated ventral tegmental area dopamine neurons using patch-clamp technology *in vitro*.

Our experiment also has some limitations. For example, our experiments used all male mice. However, many clinical drugs show sex differences,[39] and our experiments did not examine the effect of dexmedetomidine-induced sedation in mice of different sexes. Furthermore, in addition to the ventral tegmental area dopamine system, there might be other important neural systems involved in the sedation induced by dexmedetomidine, which should also be studied.

Based on our findings, dexmedetomidine may have many potential applications. It is well known that aberrant dopamine concentrations are also associated with several neurologic diseases, such as Parkinson's disease,[40] depression,[41] Alzheimer's disease,[42] and more. Whether dexmedetomidine can treat these illnesses should be the subject of future studies.

In summary, dexmedetomidine activates ventral tegmental area dopamine neurons and increases dopamine concentrations in the forebrain, which attenuates the depth of sedation in mice. This mechanism may explain rapid arousability upon dexmedetomidine sedation.

Acknowledgments

The authors thank Yulong Li, Ph.D. (State Key Laboratory of Membrane Biology, Peking University School of Life Sciences, Beijing, China), for providing DA1m virus; and Suwen Zhao, Ph.D. (School of Life Science and Technology, ShanghaiTech University, Shanghai, China) and Fang Bai, Ph.D. (School of Life Science and Technology, Shanghai Tech University, Shanghai, China), for valuable discussion and comments during revision of the manuscript.

Research Support

This work was supported by the National Natural Science Foundation of China (Beijing, China; grant Nos. 31922029, 31671086, 61890951, and 61890950 to Dr. Hu and grant No. 81701049 to Dr. Zhu.)

Competing Interests

The authors declare no competing interests.

Correspondence

Address correspondence to Dr. Hu: School of Life Science and Technology, ShanghaiTech University, Shanghai 201210, China. huji@shanghaitech.edu.cn. ANESTHESIOLOGY's articles are made freely accessible to all readers on www.anesthesiology.org, for personal use only, 6 months from the cover date of the issue.

References

1. Mason KP, O'Mahony E, Zurakowski D, Libenson MH: Effects of dexmedetomidine sedation on the EEG in children. Paediatr Anaesth 2009; 19:1175–83
2. Sleigh JW, Vacas S, Flexman AM, Talke PO: Electroencephalographic arousal patterns under dexmedetomidine xedation. Anesth Analg 2018; 127:951–9
3. Nelson LE, Lu J, Guo T, Saper CB, Franks NP, Maze M: The alpha2-adrenoceptor agonist dexmedetomidine converges on an endogenous sleep-promoting pathway to exert its sedative effects. ANESTHESIOLOGY 2003; 98:428–36
4. Zhang Z, Ferretti V, Güntan İ, Moro A, Steinberg EA, Ye Z, Zecharia AY, Yu X, Vyssotski AL, Brickley SG, Yustos R, Pillidge ZE, Harding EC, Wisden W, Franks NP: Neuronal ensembles sufficient for recovery sleep and the sedative actions of α2 adrenergic agonists. Nat Neurosci 2015; 18:553–61
5. Huupponen E, Maksimow A, Lapinlampi P, Särkelä M, Saastamoinen A, Snapir A, Scheinin H, Scheinin M, Meriläinen P, Himanen SL, Jääskeläinen S: Electroencephalogram spindle activity during dexmedetomidine sedation and physiological sleep. Acta Anaesthesiol Scand 2008; 52:289–94
6. Garrity AG, Botta S, Lazar SB, Swor E, Vanini G, Baghdoyan HA, Lydic R: Dexmedetomidine-induced sedation does not mimic the neurobehavioral phenotypes of sleep in Sprague Dawley rat. Sleep 2015; 38:73–84
7. Lin N, Vutskits L, Bebawy JF, Gelb AW: Perspectives on dexmedetomidine use for neurosurgical patients. J Neurosurg Anesthesiol 2019; 31:366–77
8. Rozet I: Anesthesia for functional neurosurgery: The role of dexmedetomidine. Curr Opin Anaesthesiol 2008; 21:537–43
9. Bekker A, Sturaitis MK: Dexmedetomidine for neurological surgery. Neurosurgery 2005; 57(1 suppl):1–10
10. Mantz J, Josserand J, Hamada S: Dexmedetomidine: New insights. Eur J Anaesthesiol 2011; 28:3–6
11. Correa-Sales C, Rabin BC, Maze M: A hypnotic response to dexmedetomidine, an alpha 2 agonist, is mediated in the locus coeruleus in rats. ANESTHESIOLOGY 1992; 76:948–52

Downloaded from http://asa2.silverchair.com/anesthesiology/article-pdf/133/2/377/514505/20200800.0-00022.pdf by guest on 13 March 2024

Copyright © 2020, the American Society of Anesthesiologists, Inc. Unauthorized reproduction of this article is prohibited.

12. Franks NP: General anaesthesia: From molecular targets to neuronal pathways of sleep and arousal. Nat Rev Neurosci 2008; 9:370–86
13. Yu X, Franks NP, Wisden W: Sleep and sedative states induced by targeting the histamine and noradrenergic systems. Front Neural Circuits 2018; 12:4
14. Wijdicks EFM: The ascending reticular activating system. Neurocrit Care 2019; 31:419–22
15. Edlow BL, Takahashi E, Wu O, Benner T, Dai G, Bu L, Grant PE, Greer DM, Greenberg SM, Kinney HC, Folkerth RD: Neuroanatomic connectivity of the human ascending arousal system critical to consciousness and its disorders. J Neuropathol Exp Neurol 2012; 71:531–46
16. Solt K, Van Dort CJ, Chemali JJ, Taylor NE, Kenny JD, Brown EN: Electrical stimulation of the ventral tegmental area induces reanimation from general anesthesia. Anesthesiology 2014; 121:311–9
17. Taylor NE, Van Dort CJ, Kenny JD, Pei J, Guidera JA, Vlasov KY, Lee JT, Boyden ES, Brown EN, Solt K: Optogenetic activation of dopamine neurons in the ventral tegmental area induces reanimation from general anesthesia. Proc Natl Acad Sci U S A 2016; 113:12826–31
18. Eban-Rothschild A, Rothschild G, Giardino WJ, Jones JR, de Lecea L: VTA dopaminergic neurons regulate ethologically relevant sleep-wake behaviors. Nat Neurosci 2016; 19:1356–66
19. Chemali JJ, Van Dort CJ, Brown EN, Solt K: Active emergence from propofol general anesthesia is induced by methylphenidate. Anesthesiology 2012; 116:998–1005
20. Solt K, Cotten JF, Cimenser A, Wong KF, Chemali JJ, Brown EN: Methylphenidate actively induces emergence from general anesthesia. Anesthesiology 2011; 115:791–803
21. Taylor NE, Chemali JJ, Brown EN, Solt K: Activation of D1 dopamine receptors induces emergence from isoflurane general anesthesia. Anesthesiology 2013; 118:30–9
22. Ihalainen JA, Tanila H: *In vivo* regulation of dopamine and noradrenaline release by alpha2A-adrenoceptors in the mouse nucleus accumbens. J Neurochem 2004; 91:49–56
23. Whittington RA, Virag L, Morishima HO, Vulliemoz Y: Dexmedetomidine decreases extracellular dopamine concentrations in the rat nucleus accumbens. Brain Res 2001; 919:132–8
24. Whittington RA, Virág L: Dexmedetomidine-induced decreases in accumbal dopamine in the rat are partly mediated via the locus coeruleus. Anesth Analg 2006; 102:448–55
25. Yuan Y, Wu W, Chen M, Cai F, Fan C, Shen W, Sun W, Hu J: Reward inhibits paraventricular CRH neurons to relieve stress. Curr Biol 2019; 29:1243–1251.e4
26. Oishi Y, Takata Y, Taguchi Y, Kohtoh S, Urade Y, Lazarus M: Polygraphic recording procedure for measuring sleep in mice. J Vis Exp 2016; 107:2–7
27. Prerau MJ, Brown RE, Bianchi MT, Ellenbogen JM, Purdon PL: Sleep neurophysiological dynamics through the lens of multitaper spectral analysis. Physiology (Bethesda) 2017; 32:60–92
28. Ran M, Wang Z, Yang H, Zhang L, Li W, Yang Q, Dong H: Orexin-1 receptor is involved in ageing-related delayed emergence from general anaesthesia in rats. Br J Anaesth 2018; 121:1097–104
29. Sun F, Zeng J, Jing M, Zhou J, Feng J, Owen SF, Luo Y, Li F, Wang H, Yamaguchi T, Yong Z, Gao Y, Peng W, Wang L, Zhang S, Du J, Lin D, Xu M, Kreitzer AC, Cui G, Li Y: A genetically encoded fluorescent sensor enables rapid and specific detection of dopamine in flies, fish, and mice. Cell 2018; 174:481–496.e19
30. Uhlén S, Dambrova M, Näsman J, Schiöth HB, Gu Y, Wikberg-Matsson A, Wikberg JE: [3H]RS79948-197 binding to human, rat, guinea pig and pig alpha2A-, alpha2B- and alpha2C-adrenoceptors. Comparison with MK912, RX821002, rauwolscine and yohimbine. Eur J Pharmacol 1998; 343:93–101
31. Hume SP, Ashworth S, Lammertsma AA, Opacka-Juffry J, Law MP, McCarron JA, Clark RD, Nutt DJ, Pike VW: Evaluation in rat of RS-79948-197 as a potential PET ligand for central alpha 2-adrenoceptors. Eur J Pharmacol 1996; 317:67–73
32. Koo JW, Mazei-Robison MS, Chaudhury D, Juarez B, LaPlant Q, Ferguson D, Feng J, Sun H, Scobie KN, Damez-Werno D, Crumiller M, Ohnishi YN, Ohnishi YH, Mouzon E, Dietz DM, Lobo MK, Neve RL, Russo SJ, Han MH, Nestler EJ: BDNF is a negative modulator of morphine action. Science 2012; 338:124–8
33. Puoliväli J, Björklund M, Holmberg M, Ihalainen JA, Scheinin M, Tanila H: Alpha 2C-adrenoceptor mediated regulation of cortical EEG arousal. Neuropharmacology 2002; 43:1305–12
34. Monti JM, Monti D: The involvement of dopamine in the modulation of sleep and waking. Sleep Med Rev 2007; 11:113–33
35. Ihalainen JA, Tanila H: *In vivo* regulation of dopamine and noradrenaline release by alpha2A-adrenoceptors in the mouse prefrontal cortex. Eur J Neurosci 2002; 15:1789–94
36. van der Zeyden M, Oldenziel WH, Rea K, Cremers TI, Westerink BH: Microdialysis of GABA and glutamate: Analysis, interpretation and comparison with microsensors. Pharmacol Biochem Behav 2008; 90:135–47
37. Clapp-Lilly KL, Roberts RC, Duffy LK, Irons KP, Hu Y, Drew KL: An ultrastructural analysis of tissue surrounding a microdialysis probe. J Neurosci Methods 1999; 90:129–42
38. Borland LM, Shi G, Yang H, Michael AC: Voltammetric study of extracellular dopamine near

Downloaded from http://asa2.silverchair.com/anesthesiology/article-pdf/133/2/377/514505/20200800.0-00022.pdf by guest on 13 March 2024

Copyright © 2020, the American Society of Anesthesiologists, Inc. Unauthorized reproduction of this article is prohibited.

microdialysis probes acutely implanted in the striatum of the anesthetized rat. J Neurosci Methods 2005; 146:149–58
39. Vutskits L, Clark JD, Kharasch ED: Reporting laboratory and animal research in anesthesiology: The importance of sex as a biologic variable. Anesthesiology 2019; 131:949–52
40. Zhuang X, Mazzoni P, Kang UJ: The role of neuroplasticity in dopaminergic therapy for Parkinson disease. Nat Rev Neurol 2013; 9:248–56
41. Nestler EJ, Carlezon WA Jr: The mesolimbic dopamine reward circuit in depression. Biol Psychiatry 2006; 59:1151–9
42. Nobili A, Latagliata EC, Viscomi MT, Cavallucci V, Cutuli D, Giacovazzo G, Krashia P, Rizzo FR, Marino R, Federici M, De Bartolo P, Aversa D, Dell'Acqua MC, Cordella A, Sancandi M, Keller F, Petrosini L, Puglisi-Allegra S, Mercuri NB, Coccurello R, Berretta N, D'Amelio M: Dopamine neuronal loss contributes to memory and reward dysfunction in a model of Alzheimer's disease. Nat Commun 2017; 8:14727

ANESTHESIOLOGY REFLECTIONS FROM THE WOOD LIBRARY-MUSEUM

Byline Backstory No. 7: Following the Historic Footsteps of Snow in Anesthesia and Public Health

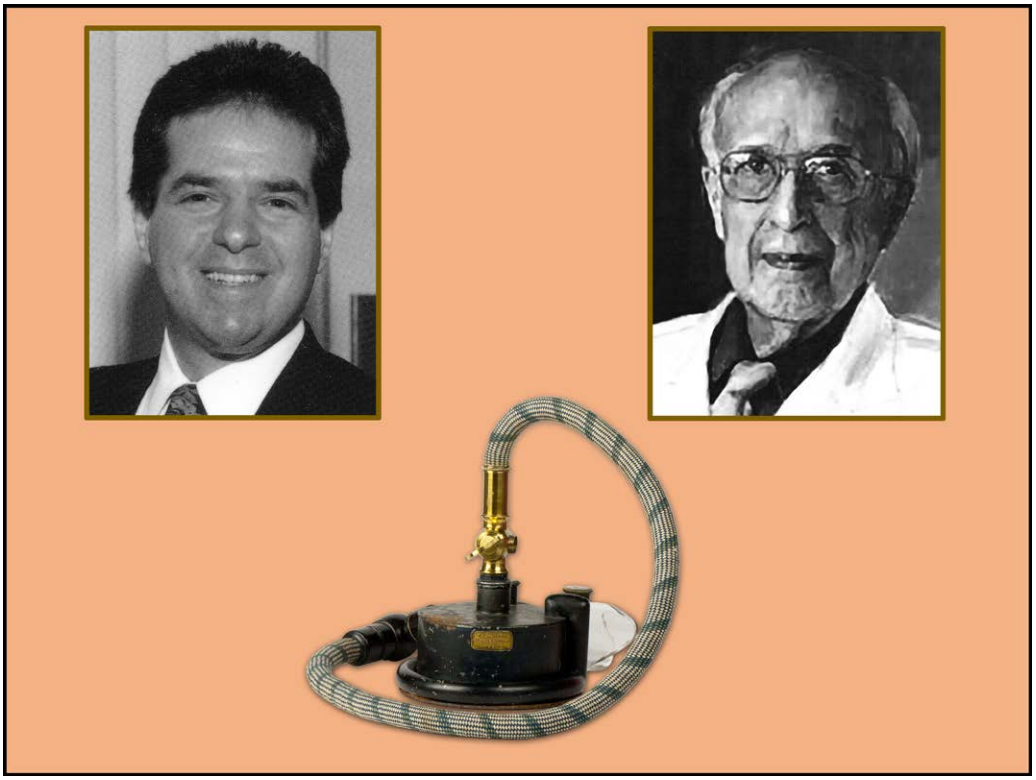

On one of my clinical rotations as a Johns Hopkins medical student, I worked alongside surgical resident Ira Rutkow, M.D., M.P.H. (*upper left*), who encouraged me to pursue the history of medicine and to follow him into Hopkins' (now Bloomberg) School of Public Health. There I met Professor George Comstock (*upper right*) who idolized John Snow, M.D., a British pioneer of both anesthesiology and epidemiology. Studying Snow's life and his ether inhaler (*bottom*) kindled my enthusiasm to pursue anesthesia history and then curate departmental anesthesia museums at Hopkins and then Yale. Examining epidemiology, the field fathered by Snow, convinced me to seek ways of reducing anesthetic morbidity and mortality in an at-risk group, the elderly. So, while Ira Rutkow was preparing himself to become America's leading surgeon-historian, I was drafting the nation's first fellowship in geriatric anesthesiology (completed 1984 to 1985), at Johns Hopkins and at the National Institutes of Health's National Institute on Aging. (Copyright © the American Society of Anesthesiologists' Wood Library-Museum of Anesthesiology.)

George S. Bause, M.D., M.P.H., Clinical Associate Professor, Case Western Reserve University, Cleveland, Ohio.

Downloaded from http://asa2.silverchair.com/anesthesiology/article-pdf/133/2/377/514505/20200800.0-00022.pdf by guest on 13 March 2024

Copyright © 2020, the American Society of Anesthesiologists, Inc. Unauthorized reproduction of this article is prohibited.